Powder Technology 323 (2018) 1–7

Contents lists available at ScienceDirect

Powder Technology

journal homepage: www.elsevier.com/locate/powtec

A comparison between interparticle forces estimated with direct powder shear testing and with sound assisted fluidization

Roberto Chirone [a], Federica Raganati [b,*], Paola Ammendola [b], Diego Barletta [c], Paola Lettieri [a], Massimo Poletto [c]

[a] Department of Chemical Engineering, University College London, Torrington Place, London WC1E 7JE, UK
[b] Istituto di Ricerche sulla Combustione (IRC), CNR, Piazzale Tecchio 80, 80125 Naples, Italy
[c] Dipartimento di Ingegneria Industriale, Università degli Studi di Salerno, Via Giovanni Paolo II, 132-84084 Fisciano (SA), Italy

ARTICLE INFO

Article history:
Received 20 April 2017
Received in revised form 18 July 2017
Accepted 21 September 2017
Available online 24 September 2017

Keywords:
Sound assisted fluidization
Fine and ultrafine cohesive powders
Interparticle forces
Cluster/subcluster model

ABSTRACT

Understanding the role of the interparticle forces in fluidization of cohesive powders is crucial for a proper application of fluidization to these type of powders. However, a direct measure of the interparticle interactions (IPFs) is challenging, mainly because cohesive particles cannot be fluidized under ordinary conditions. That is the reason why IPFs are typically measured using a rheological approach. The aim of this study is, therefore, to evaluate the IPFs of cohesive powders under actual fluidization conditions, by using an experimental and theoretical approach. In particular, a sound assisted fluidized bed apparatus was used to achieve a fluidization regime of the particles. Then, the cluster/subcluster model was applied to calculate IPFs, starting from the experimental data. The obtained IPFs were then compared to those evaluated by using a shear testing approach.

1. Introduction

In recent years an increasing numbers of industries (e.g. interested in the manufacture of cosmetics, foods, plastics, catalysts, energetic materials, biomaterials, micro-electromechanical systems [1]) have been attracted to the use of fine and ultrafine particle powders. In fact, these powders provide high specific area per unit mass [2] allowing gas solid reactions conditions offering high effectiveness of contact between phases and producing high reaction efficiencies. For these reason, it has become gradually more important to understand how to control the processes (i.e. mixing, transporting, coating) making use of these powders.

In this respect, gas fluidization is one of the most effective available techniques in ensuring continuous powder handling and dispersion characterized by good heat and mass transfer coefficients [2,3]. Because of their primary particle size and material density, fine and ultrafine powders fall under the group C (<30 μm) of the Geldart classification [4]. Powders belonging to this group are difficult to fluidize. In fact, in these powders interparticle forces (IPFs), such as van der Waals, electrostatic and moisture induced surface tension forces, can be comparable with the particle weight and the fluid dynamic forces. The relative magnitude of IPFs with respect to hydrodynamic forces (HDFs) increases as the particle size decreases [1,5]. The increased relevance of IPFs and the consequent increase of powder cohesion in group C powders determine in fluidization attempts the formation of stable gas channels when these powders are subjected to a sufficiently intense gas flow. In these conditions, the fluidizing gas bypasses the bed through the channels and the gas–solids contact efficiency results to be seriously compromised.

Clearly, understanding the role of the interparticle forces in fluidization of fine/ultrafine powders is crucial for a proper application of fluidization to fine powders. Although several studies [6–12] have been carried out on the effect of IPFs on powder fluidization, satisfactory understanding of the phenomena governing the dynamic of the bed has not yet been achieved. Most of the disagreement on the relative role of HDFs and IPFs on the fluidizability of powders sits in the complexity of the conditions that affect the intensity of IPFs that make very difficult a direct evaluation [7,13–16]. In the last years many researches have undertaken different approaches. Among these, powder flow properties measurements are a possible way to quantify interparticle forces. In particular, stationary measurements (e.g. angle of repose, Hausner ratio, see [17]) and dynamic tests [18] have been proposed as simple tests to determine and to predict the flowability of the bulk. A great number of techniques are available to characterize the flow properties at realistic process conditions, such as high temperature [19] and high humidity [20]. Moreover, different Authors [20–22] used the powder rheology as a tool to calculate indirectly the effects of the IPFs on fluidization. More recently, different groups are developing high precision fluidized bed rheometer [23,24] to directly measure the flow properties in low consolidation levels. In spite of the availability of all this tests, the relationship between the rheological properties of powders and the corresponding fluidization behaviour has not yet been achieved.

As a matter of fact, a direct measure of the particle-particle interactions and their dependency on the particle properties and on the process conditions in a fluidized bed reactor is challenging, especially

* Corresponding author.
E-mail address: f.raganati@irc.cnr.it (F. Raganati).

https://doi.org/10.1016/j.powtec.2017.09.038
0032-5910/

because fine/ultrafine particles cannot be fluidized under ordinary conditions. More specifically, because of the above-mentioned IPFs, fine/ultrafine particles are always found to be in the form of large-sized porous aggregates [25–27], rather than as individual particles, when packed together in a gaseous medium. Their fluidization actually occurs in the form of particle clusters, and their actual properties (size/density) highly affect the fluidization nature (i.e. primary particle size and density cannot be taken as representative parameters for predicting their fluidization behaviour) [2,28,29]. Accordingly, the formation of aggregates should be reduced to keep as small as possible the aggregate size in order to properly exploit the potential of fine and ultrafine particles. In other words, the achievement of a smooth fluidization regime is closely related to an efficient break-up of the large aggregates yielded by cohesive forces, thus destabilizing gas channels and enhancing the effective gas–solids contact efficiency. To this aim different assisting methods can be adopted, thus involving the application of additional forces generated, for example, by acoustic fields [2], electric fields [30], magnetic fields [31] or mechanical vibrations [32,33].

Among these, sound assisted fluidization is recognized to be one of the best alternatives. According to several works reported in literature [2,3,28,29], under the influence of appropriate acoustic fields, channeling and/or slugging tends to disappear, the bed expands uniformly and the minimum fluidization velocity is distinctly reduced. Basically, the application of the sound is associated with oscillatory gas molecule and solid particle/aggregates motion. Typically, in the case of fine/ultrafine particles the frictional force exerted on the particles by the oscillations of the gas molecules provoked by the sound wave becomes large as compared with particle inertia, thus the particles are entrained in the oscillating gas-flow field [34]. In particular, the entity of this motion is dependent on the size of particles and/or particle clusters: clearly, smaller structures are much more affected by the sound perturbation than larger aggregates are [35,36]. This different response of differently sized aggregates to the sound wave is responsible of a relative motion between them, thus inducing a dynamic break-up mechanism of larger clusters into smaller subclusters, which can be more easily fluidized. In particular, according to the theoretical cluster/subcluster oscillators model proposed by Russo et al. [36], the break-up of clusters into subclusters occurred at a contact points where the collision energy, sound energy, induced by the acoustic field exceed the particle cohesive force.

In this general framework, this work is focused on the direct evaluation of IPFs of cohesive powders under actual fluidization conditions, by using an experimental and theoretical approach. To this aim, sound assisted fluidization was used to achieve a fluidization regime of these cohesive particles. Then, using the results obtained from the experimental tests, the cluster/subcluster model was applied to calculate IPFs. The obtained IPFs were then compared to those evaluated by using a shear testing approach [19].

2. Materials and methods

2.1. Material characterization

The experimental activity was carried out on five powder samples provided by an industrial partner with different particle size distribution and same density for all the cuts. The particle size distribution was obtained by using a laser granulometer (Master-sizer 2000 Malvern Instruments), after the dispersion of the powders in water under mechanical agitation of the suspension and with the application of ultrasound (US). This system allows detection of particles in the range of 0.02–2000 μm [19].

2.2. Experimental apparatus

The laboratory scale sound-assisted fluidized bed is made of a Plexiglas column (40 mm ID and 1500 mm high) equipped with a porous gas distributor plate located at 300 mm from the bottom of the column. The section of the column below the gas distributor acts as wind-box: it is filled with Pyrex rings, thus maximizing the uniformity of the gas flow entering the fluidized bed. This solution provides a good dispersion of the fluidizing gas, thus limiting fluidization troubles due to the formation of preferential channels, namely the feed of the fluidizing gas through a limited number of points. The column is provided with a pressure probe located at the wall, 5 mm above the gas distributor, to measure the pressure drops across the bed of particles. The sound-generation system consists of a digital signal generator, a power audio amplifier rated up to 40 W and a 8 W woofer loudspeaker. More detailed information about the sound generation and insulation system can be found elsewhere [2].

The acoustic field is introduced inside the column through an ad-hoc designed sound wave guide located at the top of the freeboard [2]. The sound wave guide was properly designed to prevent the elutriated powders from dirtying the loudspeaker [2]. This experimental set-up was also designed according to the Helmholtz resonator, i.e. one of the most used engineering noise control methods, in order to reduce the sound insulation even for high intensity acoustic fields.

Gas feed is prepared using N_2 cylinders (99.995%). The flowrates were set and controlled by two mass flow controllers (Brooks 8550S).

2.3. Fluidization tests

The fluidization behaviour of all the samples was assessed under both ordinary and sound assisted conditions (sound intensity, SPL = 140–150 dB and frequency, $f = 50$–120 Hz) in the experimental apparatus described above. In particular, for each test, pressure drop curves were obtained measuring the pressure drops by both decreasing (DOWN) and increasing (UP) the superficial gas velocity. Since no remarkable differences were observed between UP and DOWN tests, only DOWN results will be reported in the following sections. All the tests were performed at ambient temperature and pressure, using N_2 as the fluidizing gas in order to prevent any intensification of the powder cohesiveness due to air moisture. For all the tests 100 g of powder were loaded in the fluidization column. For each test, pressure drop curves were obtained, i.e. the pressure drop of the gas was measured and plotted as a function of the superficial gas velocity.

The experimental pressure drop data were elaborated, by means of a graphic procedure, in order calculate the minimum fluidization velocity, u_{mf} [3], i.e. the intersection between the line fitting the data for flow through a packed bed, and a horizontal line fitting the data for the fully fluidized bed. Then, from the experimental u_{mf} the size of the fluidizing aggregates was evaluated using the correlation proposed by Wen and Yu [37]. In particular, we considered an internal voidage of 0.25 for the cohesive samples (S1, S2 and S3) to account for the apparent density of aggregate being lower than the density of the primary particles.

3. Model

The cluster/subcluster oscillator model, proposed by Russo et al. [36] to describe the fluidization of cohesive powders (i.e. belonging to the C group of Geldart's classification), was used in this work to evaluate the magnitude of the cohesive forces between fluidizing aggregates.

Russo et al. [36] interpreted the break-up of agglomerated solids in sound-assisted fluidization on the basis of two distinct physical phenomena: the hydrodynamic stresses due to gas flowing and the cohesivity of the agglomerated solids, which in turn depends both on the packing of primary particles within the agglomerate and on the strength of the elementary interparticle interaction [36].

The main assumptions of the model are:

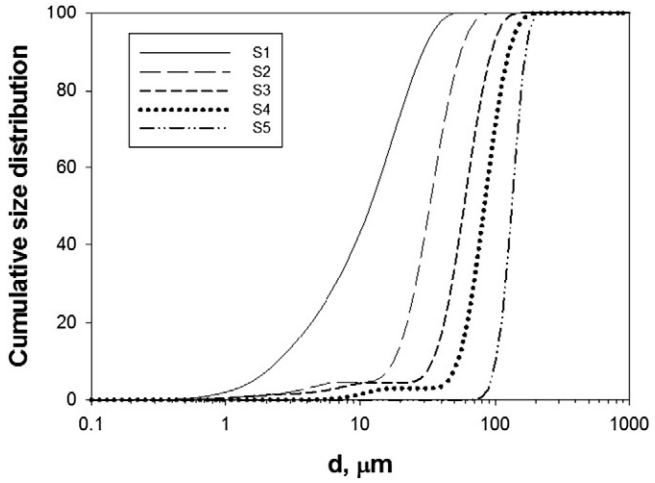

Fig. 1. Cumulative size distribution of the different samples.

(i) The existence of elastic forces between clusters and subclusters, active at the contact points, was assumed. In other words, according to this model, an elastic behaviour of the whole cluster-subcluster structure occurs as a result of the elasticity of the interparticle contacts. In particular, elastic forces are of the type kx, where k is the elastic constant relative to the force acting at each contact point between a cluster and a subcluster and x the vertical displacement of the subcluster relative to the cluster. A subcluster is in contact with the cluster at n points, so that the overall elastic constant is $[nk]$. The number of contact points is proportional to the external surface area of the subcluster.

(ii) The cohesive frictional force between a cluster and a subcluster is given by:

$$F_c = n\mu F_{cw} \tag{1}$$

where $\mu = 0.1$ is a static friction coefficient and F_{cw} is the van der Waals force along straight lines through centers of a cluster and a subcluster [36]. Even though electrostatic, capillary and van der Waals forces may develop at contact points between solids [36], only van der Waals forces are considered in the model. Electrostatic forces are disregarded because of the low velocity at which the powder has been fluidized. Capillary forces are neglected considering the low humidity of the fluidizing gas. The cohesive frictional force, F_c, tends to keep the subcluster in place.

(iii) A subcluster detaches from the cluster when the elastic force $[nk]x$ (i.e., the force that, would be necessary to keep together cluster and sublaster) is larger than the cohesive frictional force F_c, i.e. if the disaggregating force due to the application of the acoustic field, F_{sound}, is larger than the cohesive force F_c:

$$F_{sound} \geq F_c \Rightarrow [nk]|x| \geq n\mu F_{cw} \tag{2}$$

The balance of forces acting on the subcluster, taking into account inertial, elastic and drag forces, is given by:

$$m\frac{d^2x}{dt^2} + [nk]x - c_{ds}\left(U\,\sin(2\pi ft) - \frac{dx}{dt}\right) = 0 \tag{3}$$

being m the mass of the subcluster, U the amplitude of the air particle velocity, f the sound frequency and cd_s the drag force per unit gas velocity. In particular, the overall velocity of gas impinging on clusters and subclusters is the sum of two components, the upward velocity u_0 due to the gas flux for fluidization plus the velocity $U\sin(2\pi ft)$ due to sound, whereas c_{d_s} is given by:

$$c_{d_s} = 3\pi\beta\nu\rho_g d_s \tag{4}$$

where ν and ρ_g are the kinematic viscosity and the density of the gas, respectively, d_s is the subcluster diameter and $\beta = 1.7$ is a correction factor accounting for the influence of neighbouring clusters [38].

When $c_{d_s} = 0$ Eq. (3) becomes:

$$m\frac{d^2x}{dt^2} + [nk]x = 0 \tag{5}$$

By solving Eq. (5), the natural frequency of the undamped oscillator, f_n, can be evaluated:

$$f_n = \frac{1}{2\pi}\sqrt{\frac{[nk]}{m}} = \frac{1}{2\pi}\sqrt{\frac{[nk]}{(\pi/6)\rho_s d_s^3}} \tag{6}$$

Then, the overall elastic constant $[nk]$ can be expressed as:

$$[nk] = (2\pi f_n)^2 m \tag{7}$$

Substituting Eq. (7) in Eq. (3):

$$m\frac{d^2x}{dt^2} + c_{ds}\frac{dx}{dt} + (2\pi f_n)^2 mx = c_{d_s}U\sin(2\pi ft) \tag{8}$$

Then, integration of Eq. (8) leads to [39]:

$$\begin{aligned} x(t) &= \frac{U}{2\pi\sqrt{f^2 + \left(\frac{2\pi m}{c_{d_s}}\right)^2\left(f_n^2 - f^2\right)^2}}\sin(2\pi ft + \varphi) \\ &= A(f)\sin(2\pi ft + \phi) \end{aligned} \tag{9}$$

where, A is the amplitude of the displacement of the subcluster relative to the cluster, and ϕ is the phase lag between the velocity of the gas and the displacement of the subcluster:

$$\phi = \tan^{-1}\left(\frac{c_{d_s}f}{2\pi m\left(f^2 - f_n^2\right)}\right) \tag{10}$$

Then, the peak of the $A(f)$ curve occurs at the frequency f_0 which is the resonance frequency of the damped oscillator given by:

$$f_0 = f_n\left(1 - 2\left(\frac{c_{d_s}}{4\pi f_n m}\right)^2\right)^{0.5} \tag{11}$$

Combining Eq. (7) and Eq. (11), the overall elastic constant $[nk]$ can be expressed as a function of f_0:

$$[nk] = (2\pi)^2\left(f_0^2 + 2\left(\frac{c_{d_s}}{4\pi m}\right)^2\right)m \tag{12}$$

The value of the disaggregating force, F_{sound}, (i.e. the force generated by sound application) was evaluated by applying the failure conditions,

Table 1
Nominal sieving range and Sauter diameter of the powders.

Samples	Nominal sieving range μm	Sauter diameter μm
S1	<20	5.7
S2	20–38	19.0
S3	38–63	29.0
S4	63–88	65.8
S5	>88	112.3

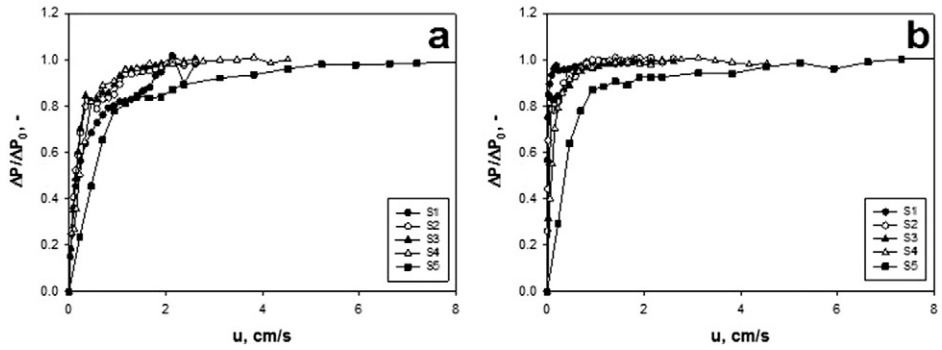

Fig. 2. Dimensionless pressure drops curves under (a) ordinary and (b) sound assisted conditions (140 dB–80 Hz).

given by Eq. (2). Therefore, F_{sound} is the disaggregating force that is necessary for subclusters of size d_s^* to detach from clusters. d_s^* was evaluated from experimental data as the size of subclusters obtainable at the maximum response frequency, f_0^*, i.e. the frequency at which, for given SPL, subclusters of minimum size d_s^* detach from clusters. The maximum response frequency is the counterpart of f_0, i.e. the resonance frequency of the subcluster behaving like a damped forced oscillator, namely $f_0 = f_0^*$.

The occurrence of the failure condition implies a tangency condition

$$[n^*k]A(f_0^*) = n^*\mu F_{cw} \tag{13}$$

Being n^* the number of active contact points between the subcluster of size d_s^* and the cluster it detaches from. Namely, F_{sound} can be evaluated using a graphical procedure as the maximum of the curve of the elastic force. In particular, the curve of the elastic force, $[n^*k]$ $A(f)$, can be plotted as a function of sound frequency. Then, the failure condition implies that the horizontal line corresponding to the cohesive forces ($n^*\mu F_{cw}$), which is independent of the sound frequency, is tangent to the maximum of the curve of elastic force. This procedure can be used to obtain the disaggregating force directly, overcoming the lack of knowledge of the number of active contact points n^*.

4. Results and discussion

4.1. Materials characterization

Fig. 1 and Table 1 report the cumulative size distribution and the Sauter diameter of all the samples, respectively. Based on their Sauter diameter (<30 μm), sample S1, S2 and S3 belongs to the C group of Geldart's classification, meaning that they are cohesive powders, i.e. their fluidization quality is expected to be poor under ordinary conditions. On the contrary, samples S4 and S5 are coarser, suggesting that their fluidization quality is expected to be good even under ordinary conditions.

4.2. Fluidization tests

Fig. 2 reports the dimensionless pressure drops ($\Delta P/\Delta P_0$ vs u) curves obtained for all the samples under ordinary and sound-assisted conditions (140 dB–80 Hz), respectively, ΔP being the actual pressure drop across the bed, ΔP_0 the pressure drop equal to buoyant weight of particles per unit area of bed. For uniform fluidization, the pressure drops are equal to the material weight per unit area (i.e. $\Delta P/\Delta P_0 = 1$), meaning that the whole bed is fluidized. As expected, samples S1, S2 and S3 are characterized by a poor fluidization quality under ordinary conditions, as confirmed by the quite irregular pressure drops curves, as typical of cohesive powders due to channeling and plugging phenomena occurring inside the bed. On the contrary, pressure drops curves obtained with the assistance of sound are far more regular, both qualitatively and quantitatively. Therefore, the application of the sound is required to achieve a proper fluidization regime. In particular, the role of the sound assistance in a fluidized bed of fine powders is to induce a continuous break-up mechanism of the large aggregates present inside the bed into smaller fluidizable ones due to the action of external (drag and inertial) forces, which counteract the internal (cohesive) forces [2].

The coarser samples, S4 and S5, in contrast, are characterized by a good fluidization under ordinary conditions and they are insensible to the application of the acoustic field.

Fig. 3 a and b report the experimental values of u_{mf} and the values of the fluidizing aggregate size of all the sample obtained under ordinary and sound assisted conditions. First of all, in contrast to their nominal size, the dimension of the fluidizing structures (and u_{mf} as a consequence) follows the order S1 > S2 > S3, in agreement with the increasing cohesive character with the powders becoming finer. Obviously, samples S4 and S5 show a more straightforward behaviour, in agreement with their nominal size.

Then, under sound assisted conditions (140 dB–80 Hz) all the cohesive samples, i.e. S1, S2 and S3, are characterized by values of u_{mf} lower than those obtained under ordinary conditions, according to the

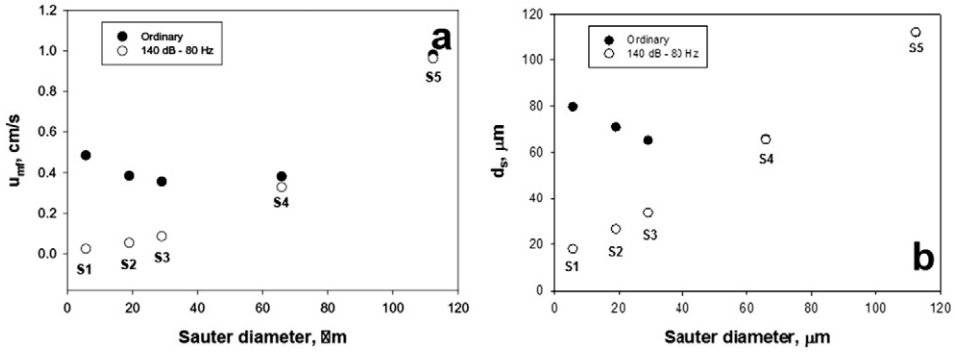

Fig. 3. (a) Experimental values of the minimum fluidization velocity and (b) fluidizing aggregate diameter for the different samples under ordinary and sound assisted fluidization conditions.

fluidization quality being enhanced by the application of the sound. This means that under ordinary conditions the fluidizing aggregates are remarkably larger than those fluidizing under sound assisted conditions, as confirmed by Fig. 3b, i.e. it can be inferred from reduction of u_{mf} that the acoustic perturbation disrupts the original clusters into smaller subclusters. Clearly, the difference observed between ordinary and sound assisted conditions tends to decrease passing from sample S1 to S2 to S3, in agreement with the reduced cohesivity with the samples becoming coarser. However, the application of an acoustic perturbation of such SPL and frequency is not enough to break up the clusters down to the Sauter diameter. Finally, as expected, samples S4 and S5 are completely unaffected by the application of the acoustic field.

Fig. 4 reports the values of the subcluster diameter as a function of SPL. As reported in literature [2], SPL has a beneficial effect on the fluidization quality of cohesive powders, indeed, d_s (and u_{mf} as a consequence) is always decreased passing from 140 to 150 dB. This evidence is due to the fact that with increasing SPLs more energy is introduced inside the bed, thus making the break-up of larger clusters more and more efficient. However, even though the increase of SPL is effective in enhancing the break-up mechanism, it is also clear that for the cohesive samples, S1, S2 and S3, not even SPLs as high as 150 dB are capable to disrupt the clusters down to the size obtained from the granulometric distribution. In addition, the gap between the size of the granulometric distribution and the actual size of the fluidizing aggregates decrease passing from the finer, S1, to the coarser cohesive sample, S3. With reference to samples S4 and S5, they fluidize in the form of particles with actual size corresponding to their Sauter diameter, regardless of the application of the sound (i.e. their fluidization behaviour is not affected by the acoustic perturbation since they are not cohesive).

With reference to the effect of sound frequency, in agreement to several works reported in literature, it has a not monotonic effect on the fluidization quality of the cohesive samples, as confirmed by the fact that the curve of u_{mf} is characterized by a minimum value at 80 Hz (f_0^*), i.e. the maximum response frequency (Fig. 5). This behaviour is due to the fact that the frequency directly affects the relative motion between clusters and subclusters, which, in turn, promotes the essential break-up and reaggregation mechanism. In particular, for too high frequencies the acoustic field cannot properly propagate inside the bed; the sound absorption coefficient is proportional to the square of sound frequency as sound propagates through the bed of particles [36]. Consequently, for too high sound frequencies, most of the acoustic energy is absorbed by the upper part of the bed (since the sound source is located at the top of the column), whereas, only an attenuated sound energy reaches the bed bottom, thus failing to efficiently disrupt large agglomerates at the bottom of the bed and, hence, fluidization quality decreases (i.e. u_{mf} increases) [40,41]. On the contrary, for too low frequencies the relative motion between larger and smaller subaggregates is practically absent. In particular, the period of the acoustic excitation is long with respect to the time needed for the flow of fluidizing gas to set up local channeling in the bed, which, after the initial perturbation, has recovered its adhesion [2]. Clearly, the fluidization quality of samples S3 and S4 is not affected by sound frequency.

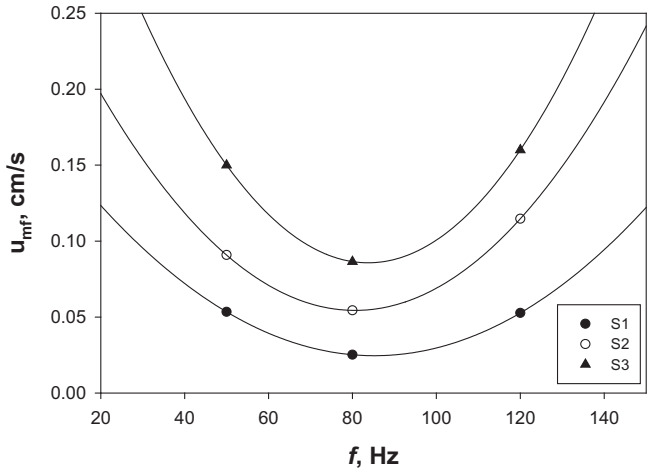

Fig. 5. Effect of sound frequency, at fixed SPL (140 dB), on u_{mf} for the cohesive samples.

5. Model application

The cluster/subcluster model was applied for the cohesive samples, S1, S2 and S3, in order to evaluate the frictional cohesive forces F_{sound}. The model was not applicable for the coarser samples, S4 and S5; since they are not cohesive, they do not fluidize under the form of aggregates and their fluidization behaviour is not affected by sound application.

The values of F_{sound} evaluated from the model are reported in Fig. 6 as a function of the SPL. It is clear that the disaggregating force due to the application of the acoustic field (i.e. the cohesive frictional force at contact points between subclusters and clusters) is enhanced with increasing values of SPL, in agreement with the experimental results obtained from the fluidization tests. Indeed, as shown in Fig. 4, increasing SPL from 140 to 150 dB results in a decrease of the fluidizing subcluster size, i.e. more energy is introduced inside the bed, thus making the break-up mechanism more efficient.

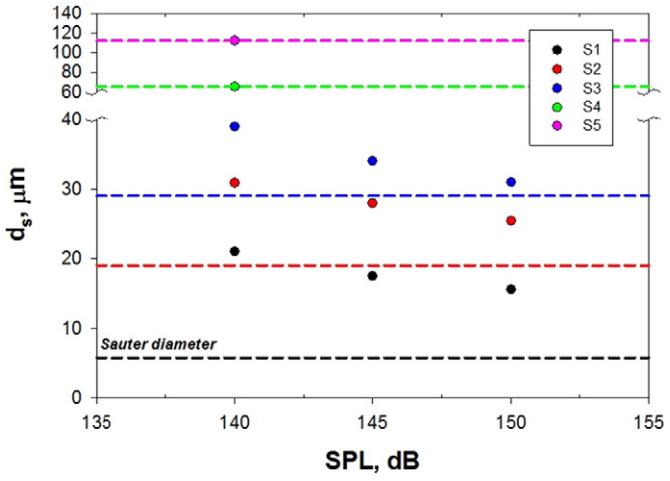

Fig. 4. Subcluster diameter as a function of the SPL for the different samples. Sauter diameters (dashed lines) of each sample are also reported.

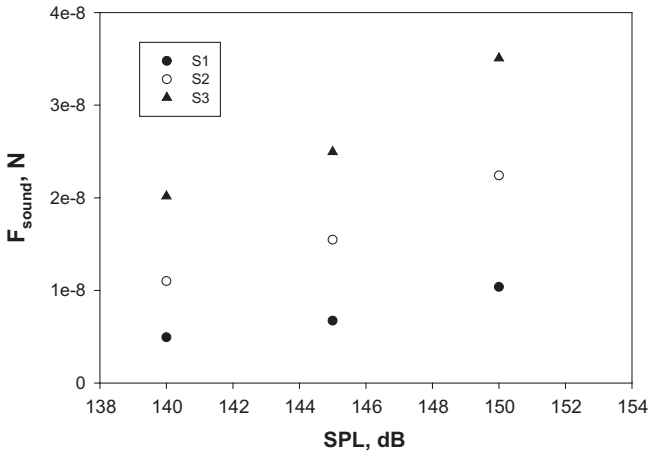

Fig. 6. Disaggregating force due to the application of the acoustic field as a function of SPL for the different samples.

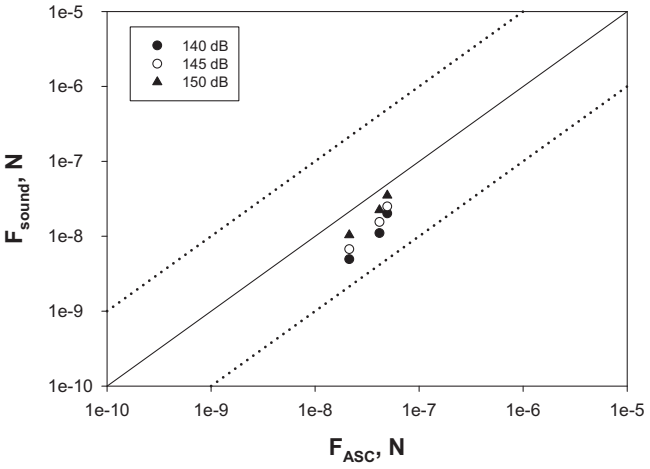

Fig. 7. Comparison between the cohesive forces evaluated in the annular shear cell (F_{ASC}) and in the sound assisted fluidized bed (F_{sound}). (Dotted lines ± one order of magnitude).

The cohesive frictional forces obtained in this work, F_{sound}, i.e. under sound assisted fluidization conditions, were then compared to those evaluated by Chirone et al. [19], i.e. through shear experiments performed in the annular shear cell (ASC) apparatus, F_{ASC}. They used the Eq. (14) proposed by Rumpf [42] and Molerus [43], which relate the tensile strength with the interparticle forces:

$$\sigma_t = \frac{F_{ASC}}{d_{sv}^2}\frac{1-\varepsilon}{\varepsilon} \tag{14}$$

where σ_t, d_{sv}, and ε are the tensile strength, the Sauter mean diameter and the bulk density, respectively. With the assumptions of Coulomb material the tensile strength has been extrapolated from the yield locus through the Eq. (15).

$$\sigma_t = \frac{C}{\tan\varphi} \tag{15}$$

The results of this comparison are shown in Fig. 7. Clearly, even though evaluated in different conditions, the values obtained are always of the same order of magnitude. To better highlight the comparison between the two approaches the ratio F_{ASC}/F_{sound} was evaluated and plotted in Fig. 8.

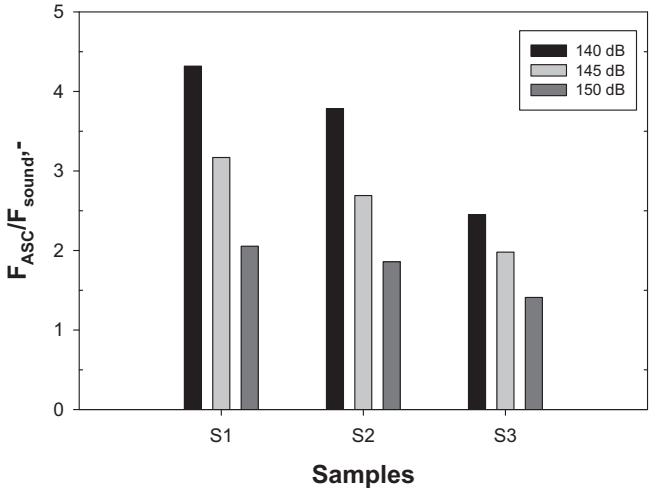

Fig. 8. Comparison between the cohesive forces evaluated in the annular shear cell (F_{ASC}) and in the sound assisted fluidized bed at different SPLs (F_{sound}).

First of all, it is clear that $F_{ASC} > F_{sound}$. This evidence is due to the fact the shear experiments in the ASC apparatus were performed in compacted conditions, which are completely different from those actually occurring inside the fluidized bed. On the contrary, in the sound assisted fluidized bed apparatus the powders are under aeration conditions; therefore, the cohesive forces are coherently lower than those evaluated in the ASC apparatus. It has to be acknowledged, however, that the material used is characterized by a rather hard material for which interparticle forces are only slightly affected by the material consolidation.

It is also clear from Fig. 8 that, for each sample, the ratio F_{ASC}/F_{sound} tends to decrease with increasing SPLs, passing from values of 2.5–4.3 down to values of 1.4–2.1. This evidence can be likely explained considering that with increasing SPLs the difference between the two evaluation approaches tends to decrease. Indeed, as shown in Fig. 4, increasing the sound pressure level from 140 to 145 dB, the acoustic field is capable of disrupting the particle aggregates more and more efficiently, i.e. approaching the nominal size obtained from the granulometric distribution that is the characteristic size used in the rheological approach.

Finally, at fixed SPL, the difference between the two approaches is larger for the smaller samples. This is in agreement with the increased cohesiveness of the samples, which means that the application of the sound is less effective, i.e. more energy is needed to disrupt the clusters into smaller subclusters.

6. Conclusions

IPFs of cohesive powders under actual fluidization conditions were evaluated, by using an experimental and theoretical approach. To this aim, sound assisted fluidization was used to achieve a fluidization regime of the particles. Then, the cluster/subcluster model was applied to calculate IPFs, starting from the experimental data. The obtained IPFs (F_{sound}) were then compared to those evaluated by using a shear testing approach (F_{ASC}).

The values obtained are always of the same order of magnitude, even though evaluated in different conditions. In particular, F_{ASC} is always slightly higher than F_{sound}, since the shear experiments in the ASC apparatus were performed in compacted conditions, i.e. completely different conditions from those actually occurring inside the fluidized bed. On the contrary, under sound assisted fluidization conditions, the powders are aerated and, therefore, the cohesive forces are reasonably smaller.

Moreover, the difference between the two evaluation approaches tends to decrease with increasing SPLs, since the acoustic field is capable of disrupting the particle aggregates more and more efficiently. As a consequence, the difference between F_{ASC} and F_{sound} is reduced.

References

[1] H. Nakamura, S. Watano, Fundamental particle fluidization behavior and handling of nano-particles in a rotating fluidized bed, Powder Technol. 183 (2008) 324–332, https://doi.org/10.1016/j.powtec.2008.01.007.
[2] F. Raganati, P. Ammendola, R. Chirone, Role of acoustic fields in promoting the gas-solid contact in a fluidized bed of fine particles, KONA Powder Part. J. 32 (2015) 23–40, https://doi.org/10.14356/kona.2015006.
[3] P. Ammendola, R. Chirone, Aeration and mixing behaviours of nano-sized powders under sound vibration, Powder Technol. 201 (2010) 49–56, https://doi.org/10.1016/j.powtec.2010.03.002.
[4] D. Geldart, Types of gas fluidization, Powder Technol. 7 (1973) 285–292, https://doi.org/10.1016/0032-5910(73)80037-3.
[5] C. Zhu, Q. Yu, R.N. Dave, R. Pfeffer, Gas fluidization characteristics of nanoparticle agglomerates, AICHE J. 51 (2005) 426–429, https://doi.org/10.1002/aic.10319.
[6] S.M.P. Mutsers, K. Rietema, The effect of interparticle forces on the expansion of a homogeneous gas-fluidized bed, Powder Technol. 18 (1977) 239–248, https://doi.org/10.1016/0032-5910(77)80014-4.
[7] O. Molerus, Interpretation of Geldart's Type A, B, C and D powders by taking into account interparticle cohesion forces, Powder Technol. 33 (1982) 81–87.
[8] K. Rietema, H.W. Piepers, The effect of interparticle forces on the stability of gas-fluidized beds—I. Experimental evidence, Chem. Eng. Sci. 45 (1990) 1627–1639, https://doi.org/10.1016/0009-2509(90)80015-7.

[9] Q.F. Hou, Z.Y. Zhou, A.B. Yu, Micromechanical modeling and analysis of different flow regimes in gas fluidization, Chem. Eng. Sci. 84 (2012) 449–468, https://doi.org/10.1016/j.ces.2012.08.051.
[10] L. Massimilla, G. Donsì, Cohesive forces between particles of fluid-bed catalysts, Powder Technol. 15 (1976) 253–260, https://doi.org/10.1016/0032-5910(76)80054-X.
[11] P. Lettieri, A study of the influence of temperature on the flow behaviour of solid materials in a gas fluidized bed, 1999.
[12] G. Bruni, P. Lettieri, D. Newton, D. Barletta, An investigation of the effect of the interparticle forces on the fluidization behaviour of fine powders linked with rheological studies, Chem. Eng. Sci. 62 (2007) 387–396, https://doi.org/10.1016/j.ces.2006.08.059.
[13] J.P.K. Seville, R. Clift, The effect of thin liquid layers on fluidisation characteristics, Powder Technol. 37 (1984) 117–129, https://doi.org/10.1016/0032-5910(84)80011-X.
[14] P.N. Rowe, L. Santoro, J.G. Yates, The division of gas between bubble and interstitial phases in fluidised beds of fine powders, Chem. Eng. Sci. 33 (1978) 133–140, https://doi.org/10.1016/0009-2509(78)85079-9.
[15] G.F. Barreto, J.G. Yates, P.N. Rowe, The measurement of emulsion phase voidage in gas fluidized beds of fine powders, Chem. Eng. Sci. 38 (1983) 345–350, https://doi.org/10.1016/0009-2509(83)80152-3.
[16] A.R. Abrahamsen, D. Geldart, Behaviour of gas-fluidized beds of fine powders part I. Homogeneous expansion, Powder Technol. 26 (1980) 35–46, https://doi.org/10.1016/0032-5910(80)85005-4.
[17] R.L. Carr, Evaluating flow properties of solids, Chem. Eng. 72 (1965) 163–168.
[18] J. Schwedes, Review on testers for measuring flow properties of bulk solids, Granul. Matter 5 (2003) 1–43, https://doi.org/10.1007/s10035-002-0124-4.
[19] R. Chirone, D. Barletta, P. Lettieri, M. Poletto, Bulk flow properties of sieved samples of a ceramic powder at ambient and high temperature, Powder Technol. 288 (2016) 379–387, https://doi.org/10.1016/j.powtec.2015.11.040.
[20] G. Landi, D. Barletta, M. Poletto, Modelling and experiments on the effect of air humidity on the flow properties of glass powders, Powder Technol. 207 (2011) 437–443, https://doi.org/10.1016/j.powtec.2010.11.033.
[21] H.O. Kono, E. Aksoy, Y. Itani, Measurement and application of the rheological parameters of aerated fine powders — a novel characterization approach to powder flow properties, Powder Technol. 81 (1994) 177–187, https://doi.org/10.1016/0032-5910(94)02876-1.
[22] G. Bruni, D. Barletta, M. Poletto, P. Lettieri, A rheological model for the flowability of aerated fine powders, Chem. Eng. Sci. 62 (2007) 397–407, https://doi.org/10.1016/j.ces.2006.08.060.
[23] M. Leturia, M. Benali, S. Lagarde, I. Ronga, K. Saleh, Characterization of flow properties of cohesive powders: a comparative study of traditional and new testing methods, Powder Technol. 253 (2014) 406–423, https://doi.org/10.1016/j.powtec.2013.11.045.
[24] H. Salehi, D. Schutz, R. Romirer, D. Barletta, M. Poletto, The Use of a Powder Rheometer to Characterize the Powder Flowability at Low Consolidation with Torque Resistances., Sumbitted to AIChEJ, 2017.
[25] G.P. Sanganwar, R.B. Gupta, A. Ermoline, J.V. Scicolone, R.N. Dave, Environmentally benign nanomixing by sonication in high-pressure carbon dioxide, J. Nanopart. Res. 11 (2009) 405–419, https://doi.org/10.1007/s11051-008-9394-z.
[26] Y. Wang, F. Wei, G. Luo, H. Yu, G. Gu, The large-scale production of carbon nanotubes in a nano-agglomerate fluidized-bed reactor, Chem. Phys. Lett. 364 (2002) 568–572.
[27] D. Barletta, M. Poletto, Aggregation phenomena in fluidization of cohesive powders assisted by mechanical vibrations, Powder Technol. 225 (2012) 93–100, https://doi.org/10.1016/j.powtec.2012.03.038.
[28] P. Ammendola, R. Chirone, F. Raganati, Effect of mixture composition, nanoparticle density and sound intensity on mixing quality of nanopowders, Chem. Eng. Process. Process Intensif. 50 (2011) 885–891, https://doi.org/10.1016/j.cep.2011.05.001.
[29] P. Ammendola, R. Chirone, F. Raganati, Fluidization of binary mixtures of nanoparticles under the effect of acoustic fields, Adv. Powder Technol. 22 (2011) 174–183, https://doi.org/10.1016/j.apt.2010.10.002.
[30] J.M. Valverde, M.J. Espin, M.A.S. Quintanilla, A. Castellanos, Electrofluidized bed of silica nanoparticles, J. Electrost. 67 (2009) 439–444, https://doi.org/10.1016/j.elstat.2009.01.021.
[31] P. Zeng, T. Zhou, J. Yang, Behavior of mixtures of nano-particles in magnetically assisted fluidized bed, Chem. Eng. Process. Process Intensif. 47 (2008) 101–108, https://doi.org/10.1016/j.cep.2007.08.009.
[32] C.H. Nam, R. Pfeffer, R.N. Dave, S. Sundaresan, Aerated vibrofluidization of silica nanoparticles, AICHE J. 50 (2004) 1776–1785, https://doi.org/10.1002/aic.10237.
[33] D. Barletta, P. Russo, M. Poletto, Dynamic response of a vibrated fluidized bed of fine and cohesive powders, Powder Technol. 237 (2013) 276–285, https://doi.org/10.1016/j.powtec.2012.12.004.
[34] J.M. Valverde, F. Raganati, M.A.S. Quintanilla, J.M.P. Ebri, P. Ammendola, R. Chirone, Enhancement of CO_2 capture at Ca-looping conditions by high-intensity acoustic fields, Appl. Energy 111 (2013) 538–549, https://doi.org/10.1016/j.apenergy.2013.05.012.
[35] R. Chirone, L. Massimilla, S. Russo, Bubble-free fluidization of a cohesive powder in an acoustic field, Chem. Eng. Sci. 48 (1993) 41–52.
[36] P. Russo, R. Chirone, L. Massimilla, S. Russo, The influence of the frequency of acoustic waves on sound-assisted fluidization of beds of fine particles, Powder Technol. 82 (1995) 219–230, https://doi.org/10.1016/0032-5910(94)02931-D.
[37] C.Y. Wen, Y.H. Yu, A generalized method for predicting the minimum fluidization velocity, AICHE J. 12 (1966) 610–612, https://doi.org/10.1002/aic.690120343.
[38] M.E. O'Neill, A sphere in contact with a plane wall in a slow linear shear flow, Chem. Eng. Sci. 23 (1968) 1293–1298, https://doi.org/10.1016/0009-2509(68)89039-6.
[39] W. Flugge, Handbook of Engineering Mechanics, McGrawHill, New York, 1963.
[40] F. Raganati, P. Ammendola, R. Chirone, Effect of acoustic field on CO2 desorption in a fluidized bed of fine activated carbon, Particuology 23 (2015) 8–15, https://doi.org/10.1016/j.partic.2015.02.001.
[41] P. Ammendola, F. Raganati, R. Chirone, Effect of operating conditions on the CO2 recovery from a fine activated carbon by means of TSA in a fluidized bed assisted by acoustic fields, Fuel Process. Technol. 134 (2015) 494–501, https://doi.org/10.1016/j.fuproc.2015.03.010.
[42] H. Rumpf, Zur Theorie der Zugfestigkeit von Agglomeraten bei Kraftübertragung an Kontaktpunkten, Chemie Ing. Tech. 42 (1970) 538–540, https://doi.org/10.1002/cite.330420806.
[43] O. Molerus, Theory of yield of cohesive powders, Powder Technol. 12 (1975) 259–275, https://doi.org/10.1016/0032-5910(75)85025-X.